Rapid Induction of Dopaminergic Neuron Loss Accompanied by Lewy Body-Like Inclusions in A53T BAC-SNCA Transgenic Mice

Shinya Okuda
Kyoto University Graduate School of Medicine Faculty of Medicine: Kyoto Daigaku Daigakuin Igaku Kenkyuka Igakubu https://orcid.org/0000-0002-1444-9381

Norihito Uemura (nuemura@kuhp.kyoto-u.ac.jp)
Kyoto University Graduate School of Medicine https://orcid.org/0000-0002-6251-0810

Masanori Sawamura
Kyoto University Graduate School of Medicine Faculty of Medicine: Kyoto Daigaku Daigakuin Igaku Kenkyuka Igakubu

Tomoyuki Taguchi
Kyoto University Graduate School of Medicine Faculty of Medicine: Kyoto Daigaku Daigakuin Igaku Kenkyuka Igakubu

Masashi Ikuno
Kyoto University Graduate School of Medicine Faculty of Medicine: Kyoto Daigaku Daigakuin Igaku Kenkyuka Igakubu

Maiko T. Uemura
Kyoto University Graduate School of Medicine Faculty of Medicine: Kyoto Daigaku Daigakuin Igaku Kenkyuka Igakubu

Hodaka Yamakado
Kyoto University Graduate School of Medicine Faculty of Medicine: Kyoto Daigaku Daigakuin Igaku Kenkyuka Igakubu

Ryosuke Takahashi
Kyoto University Graduate School of Medicine Faculty of Medicine: Kyoto Daigaku Daigakuin Igaku Kenkyuka Igakubu

---

Research article

Keywords: Parkinson's disease, propagation, dopaminergic neurons, Lewy bodies, α-Synuclein, transgenic mouse, behavioral abnormalities

Posted Date: April 2nd, 2021

DOI: https://doi.org/10.21203/rs.3.rs-355605/v1

Version of Record: A version of this preprint was published at Neurotherapeutics on December 21st, 2021.
See the published version at https://doi.org/10.1007/s13311-021-01169-5.

Abstract

Background

Parkinson's disease (PD) is the most common neurodegenerative movement disorder. Pathological features of PD include dopaminergic neuron loss in the substantia nigra pars compacta (SNpc) and intraneuronal α-Synuclein (α-Syn) inclusions called Lewy bodies (LBs). Since there is no treatment to either halt or slow the progression of PD, it is highly demanded to establish a rodent model that recapitulates the clinicopathological features of PD within a short period to efficiently investigate the pathological mechanisms and test disease-modifying therapies (DMTs).

Methods

We injected human and mouse α-Syn-preformed fibrils (hPFFs and mPFFs, respectively) into the hemilateral dorsal striatum of wild-type mice, wild-type human α-Syn bacterial artificial chromosome (BAC) transgenic (WT BAC-*SNCA* Tg) mice, and A53T human α-Syn BAC transgenic (A53T BAC-*SNCA* Tg) mice, and conducted pathological and behavioral analyses.

Results

WT BAC-*SNCA* Tg and A53T BAC-*SNCA* Tg mice expressed a comparable amount of α-Syn (2.9 and 2.7-fold more α-Syn, respectively, than wild-type mice) in the brains. mPFF injections induced more severe α-Syn pathology in most brain regions, including the ipsilateral SNpc, than hPFF injections in all genotypes at 1 month post-injection. Among the mPFF-injected mice, the A53T BAC-*SNCA* Tg mice exhibited the most severe α-Syn pathology as early as 0.5 month (2 weeks) post-injection. Consistent with these observations, *in vitro* fibrillization assay revealed that a mixture of A53T human α-Syn and mouse α-Syn seeded with mPFFs aggregated most rapidly among the conditions tested. The mPFF-injected A53T BAC-*SNCA* Tg mice showed a 38% reduction in tyrosine hydroxylase (TH)-positive neurons in the ipsilateral SNpc, apomorphine-induced rotational behavior, and motor dysfunction at 2 months post-injection. Notably, the reduction in TH-positive density in the striatum and microglial activation preceded the obvious TH-positive neuron loss in the SNpc.

Conclusions

Our data indicate that the extent of α-Syn pathology induced by α-Syn PFF injection depends on the types of α-Syn PFFs and exogenously expressed α-Syn in Tg mice. The mPFF-injected A53T BAC-*SNCA* Tg mice recapitulate the pathological processes of PD more rapidly than previously reported mouse models, suggesting their usefulness for testing DMTs as well as analyzing the pathological mechanisms.

Background

Parkinson's disease (PD) is the most common neurodegenerative movement disorder [1]. The pathological findings include the loss of dopaminergic neurons in the substantia nigra pars compacta

(SNpc) and the presence of α-Synuclein (α-Syn) inclusions in the form of Lewy bodies (LBs) and Lewy neurites. Clinically, dopamine depletion in the nigrostriatal system causes motor symptoms, which can be partially relieved by dopamine replacement therapy. Although this symptomatic therapy is initially effective for motor symptoms, most patients suffer from treatment-resistant motor symptoms, dysphagia, autonomic failure, psychosis, and dementia years after the onset of PD [1, 2]. The pathological changes are also relentlessly progressive, seemingly associated with the progression of clinical symptoms. For instance, the motor dysfunction scores of the Unified Parkinson's Disease Rating Scale (UPDRS) linearly related to the neuronal density in the SNpc, which decreases with time [3]. Lewy pathology is also seen in the widespread brain regions in the late stage of PD, and its severity in the cortical areas and hippocampus correlates with cognitive decline in PD [4–6]. Thus, one of the greatest unmet therapeutic needs in PD is the development of disease-modifying therapies (DMTs) that could slow down the disease progression or change the course of the disease.

To date, all attempts to develop DMTs have failed. One of the biggest reasons for the past failures is the discrepancy between human PD and the animal models used for testing the candidate drugs. Toxin-based animal models, i.e., animals administered with 1-methyl-4-phenyl-1,2,3,6-tetrahydropyridine or 6-hydroxydopamine, which rapidly induce dopaminergic neuron loss, have been often used to identify the potential DMTs [7, 8]. However, their neurotoxic mechanisms are distinct from α-Syn–induced cellular dysfunction and death. Indeed, only a few of the candidates identified in toxin-based animal models are still considered to have a potential for disease modification [7]. Meanwhile, certain point mutations in the α-Syn gene (*SNCA*) and genomic duplication and triplication that contain the *SNCA* locus lead to autosomal dominant familial PD [9–12]. Based on these genetic findings, many α-Syn transgenic rodent models have been generated to recapitulate the α-Syn–driven pathological changes in PD [7, 13]. Although these models have enhanced our understanding of fundamental pathological processes of PD, their usage has limitations for the development of DMTs: none of them exhibit α-Syn aggregation followed by dopaminergic neuron loss in the SNpc or behavioral abnormalities within several months of age [7]. To overcome their shortcomings, viral vector-based α-Syn overexpressing rodent models have been also generated [14, 15]. They show PD-like phenotypes on the scale of weeks, the timeframes applicable to drug discovery. However, one criticism is that this is only achieved with extremely high α-Syn expression levels (several to 20 times higher than the endogenous level), which far exceed both physiological and disease conditions.

Growing evidence suggests that pathological α-Syn aggregates behave in a prion-like manner in terms of templated fibrilization and intercellular dissemination [16]. Injection of α-Syn-preformed fibrils (PFFs) into animals induces this process, formation of LB-like inclusions, and their subsequent intercellular spread [17, 18]. Particularly, striatal injection of α-Syn PFFs recapitulates the features characteristic of PD, i.e., the formation of LB-like inclusions followed by dopaminergic neuron loss in the SNpc and motor dysfunction [17]. However, these features take 6 months to develop in wild-type (WT) mice, which is too long for evaluating potential therapeutic effects.

We previously generated bacterial artificial chromosome (BAC) transgenic (Tg) mice harboring human α-Syn gene (*SNCA*) and *SNCA* with an A53T mutation (hereafter, WT BAC-*SNCA* Tg mice and A53T BAC-*SNCA* Tg mice, respectively) [19, 20]. The WT BAC-*SNCA* Tg mice did not exhibit any PD-related pathological or behavioral phenotypes, whereas the A53T BAC-*SNCA* Tg mice exhibited REM sleep behavior disorder (RBD)-like behavior and hyposmia, both of which are prodromal symptoms of PD, with proteinase K-resistant α-Syn aggregation and slight dopaminergic neuron loss (17% at 18 months of age compared with that of age-matched WT mice). In the present study, we applied striatal injection of human and mouse α-Syn PFFs (hPFFs and mPFFs, respectively) to these two *SNCA* Tg mouse lines to generate a novel mouse model showing key pathological and behavioral phenotypes of PD within a short period amenable to a rapid investigation of the pathological mechanisms and drug testing.

Methods

Animals and ethics statement

WT (hereafter non-transgenic [nTg]) mice, homozygous WT BAC-*SNCA* Tg mice, and heterozygous A53T BAC-*SNCA* Tg mice with C57BL/6J background were used for this study. To genotype the progeny of WT BAC-*SNCA* Tg mice and A53T BAC-*SNCA* Tg mice, polymerase chain reaction was performed as described previously [20]. All experiment procedures were in accordance with the national guidelines. The Animal Research Committee of Kyoto University granted ethical approval and permission (MedKyo 17184).

Western blot analysis

Western blot analyses were conducted as described previously [21]. Briefly, phosphate buffer saline (PBS)-perfused brains were homogenized in 10 volumes (w/v) of 2% sodium dodecyl sulfate (SDS) buffer (150 mM NaCl, 1mM ethylenediaminetetraacetic acid, 10 mM Tris-HCl, 1% [v/v] Triton X-100, 2% [v/v] SDS) on ice, followed by sonication with a Bioruptor ultrasonic wave disruption system for 1 min and centrifugation at 20,400 g at 4°C for 15 min. The supernatant was boiled in sample buffer (1% [w/v] SDS, 12.5% [w/v] glycerol, 0.005% [w/v] bromophenol blue, 2.5% [v/v] 2-mercaptoethanol, 25 mM Tris-HCl, pH 6.8). Samples containing 18 μg of protein were loaded in each lane and separated on NuPAGE 4–12% (w/v) gradient gels (Invitrogen). Proteins were transferred to polyvinylidene difluoride membranes with a Trans-Blot SD Semi-Dry Transfer Cell (Bio-Rad). The membranes were treated with 4% (w/v) paraformaldehyde (PFA) in PBS for 30 min at room temperature before blocking to prevent detachment of α-Syn from the blotted membrane. For western blot analysis, the following primary antibodies were used: anti-human α-Syn (Invitrogen, #180215 [LB509], 1:500), anti-α-Syn (BD Transduction, #610787 [Syn-1], 1:2000), and anti-β-actin (Sigma-Aldrich, #A1978, 1:5000). After blocking with 5% (w/v) skim milk in PBS for 30 min, the membranes were incubated with primary antibodies at 4°C for 1 to 3 d, followed by reaction with horseradish peroxidase-conjugated secondary antibodies (Rockland Immunochemicals, TrueBlot ULTRA) for 1 h. Immunoreactive bands were detected with Chemi-Lumi One Super (Nacalai tesque), and the chemiluminescent signal was detected with Amersham Imager 600 (GE Healthcare). Densitometric analyses were performed using ImageJ software (National Institutes of Health).

Generation of α-Syn monomer and PFFs

α-Syn monomer and PFFs were generated as described previously with minor modifications [22, 23]. Briefly, mouse α-Syn and WT or A53T human α-Syn were expressed in Escherichia coli BL21 (DE3) (BioDynamics Laboratory) and were purified by boiling and ion exchange using Q sepharose fast flow (GE Healthcare). After dialyzed against dialysis buffer (150 mM KCl, 50 mM Tris-HCl, pH 7.5), α-Syn solution (7 mg/ml) was agitated at 37°C at 1,000 rpm for 10 d. After ultracentrifugation at 186,000 g at 20°C for 20 min, the pellets of α-Syn PFFs were resuspended in PBS (2.5 μg/μl) and then sonicated with a Bioruptor ultrasonic wave disruption system for 5 min before injections. The characterization of α-Syn PFFs before and after sonication was described previously [23, 24].

Stereotaxic surgery

Mice at 2–3 months of age were anesthetized with avertin (2,2,2-tribromoethanol) and then stereotaxically inoculated with 2 μl of α-Syn PFFs or PBS into the left dorsal striatum (coordinates: 0.2 mm relative to the bregma; 2.0 mm from the midline, −2.6 mm from the scull surface) using a 33-gauge Neuros syringe (Hamilton).

Immunohistochemical analysis

Mice were anesthetized with sevoflurane and transcardially perfused with 4% (w/v) PFA in PBS. The brains were removed and immersed in 4% (w/v) PFA in PBS at 4°C overnight. Paraffinized brains were sectioned with a thickness of 8 μm. For immunohistochemical and immunofluorescent analyses, the following primary antibodies were used: anti-phosphorylated-α-Syn (p-α-Syn) (Abcam, #ab51253 [EP1536Y], 1:5000), anti-p-α-Syn (Wako, #015-25191 [#64], 1:1000), anti-tyrosine hydroxylase (TH, Millipore, #MAB318 [LNC1], 1:5000), anti-TH (Millipore, #AB152, 1:500), anti-p62 (MBL, #PM045, 1:1000), anti-ubiquitin (DAKO, #Z0458, 1:1000), anti-ionized calcium-binding adapter molecule 1 (Iba1, Wako, #019-19741, 1:100), and anti-glial fibrillary acidic protein (GFAP, Sigma-Aldrich, #G3893, 1:500). The sections were incubated at 4°C with the primary antibodies for 1 to 2 d and then processed for visualization. As secondary antibodies, Histofine (Nichirei Bioscience) and Alexa Fluor 488 or 594-conjugated antibodies (Invtrogen) were used for diaminobenzidine staining and immunofluorescence, respectively. To evaluate p-α-Syn–positive pathology and the number of dopaminergic neurons in the SNpc, every 10^{th} section was stained with the anti-p-α-Syn (EP1536Y) and anti-TH (LNC1) antibodies. The numbers of p-α-Syn–positive and TH-positive cells with visible nuclei were manually counted. Semiquantitative analyses were performed on seven coronal sections (2.96, 1.34, 0.14, −1.82, −2.92, −3.88, and −5.34 mm relative to bregma), and color coded onto heat maps. The extent of p-α-Syn–positive pathology was graded as sparse to severe pathology based on the following criteria; sparse, neuritic pathology or 2–3 LB-like inclusions; mild, 4–9 LB-like inclusions; moderate, 10–29 LB-like inclusions; severe, 30 or more LB-like inclusions seen with a 20× objective lens. Scores were determined by the observations of at least 2 mice for each group. To assess microglial activation and reactive astrogliosis, the percentage of Iba1- and GFAP-positive areas in the ipsilateral SNpc were measured with

ImageJ (National Institutes of Health). For assessment of nigrostriatal dopaminergic neuron terminals, the TH optical density in the dorsal striatum at −0.22 mm, 0.26 mm, and 0.74 mm relative to the bregma was measured with ImageJ.

In vitro α-Syn fibrillization assay

In vitro α-Syn fibrillization assay was performed as described previously [25]. Briefly, a mixture consisting of mouse α-Syn monomer (0.5 mg/ml), WT or A53T human α-Syn monomer (0.5 mg/ml), and 0.5 μM thioflavin T were seeded with 1% (w/w) hPFF or mPFF, and then continuously agitated at 600 rpm. The fluorescence at 535 nm (excitation 450 nm) was measured every 0.5 h with a multi-label plate reader (PerkinElmer, 2030 ARVO X3). The initiation and elongation rates were defined as the inverse values of time to reach 25% and time from 25% to 75% of maximum thioflavin T fluorescence, respectively.

Behavioral analysis

Behavioral analyses were conducted as described previously [26]. Male mice were used for all the behavioral analyses. For the comparisons among PBS-injected nTg mice, PBS-injected A53T BAC-*SNCA* Tg mice, and mPFF-injected A53T BAC-*SNCA* Tg mice, a batch composed of 12, 13, and 13 mice, respectively, was subjected to the behavioral tests at 2 months post-injection. Before every test, the mice were habituated to the experimental environment for more than 30 min.

Apomorphine-induced rotational behavior test

Apomorphine-induced rotational behavior test was performed as previously described with minor modifications [27]. Mice received a subcutaneous injection of apomorphine (0.75 μg/g [body weight]) and were placed in an opaque cylinder of 30-cm diameter. After a 5 min habituation period, movements were recorded for 5 min. Both contralateral and ipsilateral full-body rotations are measured.

Muscular strength test

For the grip strength test, mice were lifted and held by their tail so that they grasped the wire grid of the grip strength meter (O'Hara & Co.) with their forepaws. The mice were then gently pulled backward by their tail with the posture horizontal until they released the grid. The greatest peak force measured among three tests was used for statistical analysis. For the wire hang test, mice were placed on a wire mesh, which was inverted and waved gently so that the mice gripped the wire. The latency to fall was recorded, with a 120-s cut-off time.

Elevated plus maze test

The elevated plus maze apparatus (O'Hara & Co.) consisted of two open arms (25 cm × 5 cm) and two enclosed arms of the same size with transparent walls. The arms were elevated to a height of 55 cm above the floor. Mice were placed in the central square of the maze (5 cm × 5 cm) and allowed to move

freely for 10 min. The distance traveled, entries into the arms, and time spent in the arms, were recorded automatically.

Light/dark transition test

The apparatus for the light/dark transition test consisted of a cage (42 × 21 × 25 cm) divided into two sections of equal size by a partition with a door (O'Hara & Co.). One chamber was brightly illuminated (390 lux), whereas the other chamber was dark (2 lux). Mice were placed into the dark area and allowed to move freely between the two chambers through the open door for 10 min. The transitions between chambers, time spent in each chamber, and distance traveled were recorded automatically.

Open field test

Mice were placed at the center of the field inside an open field apparatus (Accuscan Instruments, 42 × 42 × 30 cm) and allowed to move freely for 30 min. The distance traveled, time spent in the center area (20 × 20 cm), vertical activity, and stereotypic movements were recorded automatically.

Rotarod test

The accelerating rotarod (Ugo Basile) was used for the rotarod test. The speed of the rotarod accelerated from 4 to 40 rpm over a 5-min period. Mice were placed on rotating drums (3 cm diameter), and the latency to fall was recorded. Mice were subjected to the test three times a day for two consecutive days.

Porsolt forced swim test

The apparatus for the Porsolt forced swim test consisted of four Plexiglas cylinders (20 cm height × 10 cm diameter). The cylinders were filled with water (23°C), up to a height of 7.5 cm. Mice were placed in the cylinders and allowed to move freely for 10 min. The immobile time and distance traveled were recorded automatically.

Y-maze test

Mice were placed at the end of one arm of the Y-maze apparatus (O'Hara & Co.) and allowed to move freely for 5 min. The distance traveled and series of arm entries were recorded. An alternation was defined as entries into all three arms on consecutive occasions. The number of maximum alternations was therefore the total number of arm entries minus two, and the percentage of alternations was calculated.

Tail suspension test

Mice were suspended 30 cm above the floor in a visually isolated area by adhesive tape placed ~1cm from the tip of the tail. The immobile time was recorded for 10 min.

Contextual and cued fear conditioning test

On day 1, conditioning was performed. Mice were placed in a test chamber inside a sound-attenuated chamber and allowed to explore freely for 2 min. A 55-dB white noise, which is conditioned stimulus (CS), was presented for 30 s, followed by a foot shock (2 s, 0.35mA) serving as unconditioned stimulus (US). Two more CS-US parings were supplied with 2-min interstimulus intervals. On day 2, contextual memory retention test was performed 24 h after conditioning in the same chamber. The immobile time and distance traveled were recorded automatically for 5 min. On day 3, auditory-cued fear retention test under altered context was performed in a different chamber. Mice were allowed to move freely for 3 min, and then CS was presented for 3 min. The immobile time and distance traveled were recorded automatically.

Statistical analysis

Statistical calculations were performed with GraphPad Prism software, Version 5.0. All the statistical tests conducted are described in the figure legends. An F test, a Brown–Forsythe test, and a Bartlett's test were performed to evaluate the differences in variances. Differences with *p* values of less than 0.05 were considered significant.

Results

WT BAC-SNCA Tg mice and A53T BAC-SNCA Tg mice express an almost equal amount of α-Syn in the brains

In the present study, we used two *SNCA* Tg mouse lines, i.e., WT BAC-*SNCA* Tg mice and A53T BAC-*SNCA* Tg mice, both of which we generated previously [19, 20]. We used WT BAC-*SNCA* Tg and A53T BAC-*SNCA* Tg mice in homozygous and heterozygous states, respectively, because the latter line rarely produced homozygous Tg pups. We examined α-Syn expression in the brains of these BAC-*SNCA* Tg mice as well as nTg mice. These two *SNCA* Tg mouse lines expressed an almost equal amount of human and total α-Syn in their brains, with the total α-Syn overexpressed by 2.9 and 2.7-fold in WT BAC-*SNCA* Tg and A53T BAC-*SNCA* Tg mice, respectively, relative to nTg mice (Fig. 1). The amount of total α-Syn that heterozygous A53T BAC-*SNCA* Tg mice expressed as compared with that of nTg mice was higher than what we reported previously, possibly because of the difference in detergent used to extract proteins (i.e., 1% Triton X-100 buffer for the previous studies [20, 26] and 2% SDS buffer for the present study).

Comparisons of pathological changes among hPFF-, mPFF-, and PBS-injected mice at 1 month post-injection

The efficiency of templated fibrillization of α-Syn is affected by the species of both monomeric α-Syn substrate and fibrillar α-Syn seed. Seeded fibrillization of α-Syn across species is generally inefficient, which may be attributed to mismatches in amino acid sequences [25]. Because it remains unclear which fibrillar α-Syn seed more efficiently induces fibrillization in *SNCA* Tg mouse lines, we injected hPFFs, mPFFs, or PBS into the hemilateral dorsal striatum of nTg mice, WT BAC-*SNCA* Tg mice, and A53T BAC-*SNCA* Tg mice. First, we conducted pathological analyses on all the groups at 1 month post-injection. P-α-Syn immunohistochemistry revealed stronger p-α-Syn immunoreactivity in the Tg mice injected with PBS

than that in the nTg mice injected with PBS in some brain regions (Fig. 2a, Additional file 1: Figure S1). However, α-Syn PFF–induced α-Syn inclusions were clearly distinguished based on its even stronger p-α-Syn staining intensity and morphology, as we reported previously [26]. The pathological analysis revealed that p-α-Syn–positive inclusions in widespread brain regions of both hPFF- and mPFF-injected mice (Fig. 2a, f, Additional file 1: Figure S1). mPFF-injected mice were found to show comparable to more severe α-Syn pathology in most brain regions compared with hPFF-injected mice in all the genotypes (Fig. 2f). Specifically, the number of p-α-Syn–positive cells in the ipsilateral SNpc was higher in mPFF-injected mice than that in hPFF-injected mice in all the genotypes despite no significant differences among the mPFF-injected groups (Fig. 2b). We confirmed that p-α-Syn–positive inclusions seen in the ipsilateral SNpc were within TH-positive neurons (Fig. 2c). Moreover, most of the p-α-Syn inclusions were immunopositive for p62 and ubiquitin (Additional file 2: Figure S2), both of which are also positive in LBs. Since mPFF-injected mice showed more severe α-Syn pathology than hPFF-injected mice in all the genotypes, we then evaluated neuron loss in the SNpc of mPFF-injected mice by counting the number of TH-positive neurons (Fig. 2d, e). mPFF-injected nTg and WT BAC-*SNCA* Tg mice did not show neuron loss in the ipsilateral SNpc, whereas mPFF-injected A53T BAC-*SNCA* Tg mice showed significant neuron loss compared with the contralateral SNpc (Fig. 2e).

Collectively, injection of mPFFs induced more severe α-Syn pathology in all the genotypes at 1 month post-injection than that of hPFFs. Among mPFF-injected mice, A53T BAC-*SNCA* Tg mice showed significant neuron loss in the ipsilateral SNpc as early as 1 month post-injection.

Rapid formation of α-Syn pathology in mPFF-injected A53T BAC-SNCA Tg mice

Although the severity of α-Syn pathology is similar between mPFF-injected WT BAC-*SNCA* Tg and A53T BAC-*SNCA* Tg mice at 1 month post-injection, neuron loss was already seen in the latter mice at the time point (Fig. 2e). These observations prompted us to go back to an earlier time point to see the extent of α-Syn pathology with less neuron loss. The pathological analysis of mPFF-injected mice at 0.5 month (2 weeks) post-injection clearly showed more severe α-Syn pathology in most brain regions in the mPFF-injected A53T BAC-*SNCA* Tg mice than those in the mPFF-injected nTg and WT BAC-*SNCA* Tg mice (Fig. 3a–c). These results suggest that mPFF injection induces a more rapid formation of α-Syn pathology and subsequent neuron loss in A53T BAC-*SNCA* Tg mice than those in nTg and WT BAC-*SNCA* Tg mice [28]. Indeed, the α-Syn pathology was less severe in most brain regions of the mPFF-injected A53T BAC-*SNCA* Tg mice at 1 month post-injection than at 0.5 month post-injection (Fig. 2f, 3c).

In vitro fibrillization assay replicates the rapid formation of α-Syn pathology in mPFF-injected A53T BAC-SNCA Tg mice

To analyze the kinetics of α-Syn fibrillization in the conditions that recapitulate the BAC-*SNCA* Tg mice injected with α-Syn PFFs, we conducted an *in vitro* α-Syn fibrillization assay. We prepared two α-Syn monomer mixtures: one was a mixture of mouse and WT human α-Syn monomers that represent WT BAC-*SNCA* Tg mice, and the other was a mixture of mouse and A53T human α-Syn monomers that represent A53T BAC-*SNCA* Tg mice. After seeded with hPFFs or mPFFs, they were constantly agitated,

and the fluorescence of thioflavin T was monitored as the extent of α-Syn fibrillization. The mixture of mouse and A53T human α-Syn monomers seeded with mPFFs showed the most rapid initiation and elongation of α-Syn fibrillization among the conditions tested (Fig. 4a–d), which is consistent with the results of the BAC-*SNCA* Tg mice injected with α-Syn PFFs.

Pathological characterization of mPFF-injected A53T BAC-SNCA Tg mice

The results we obtained so far indicate that mPFF-injected A53T BAC-*SNCA* Tg mice have the potential as a novel PD mouse model that fulfills the purpose of this study. Therefore, we conducted pathological analyses up to 4 months post-injection to further characterize this model. The number of p-α-Syn–positive cells in the ipsilateral SNpc was the highest at 0.5 month post-injection and decreased over time, reaching almost zero at 4 months post-injection (Fig. 5a, d). The number of TH-positive neurons in the ipsilateral SNpc also decreased over time, reaching 38% and 46% reductions at 2 and 4 months post-injection, respectively (Fig. 5b, e). Interestingly, the sum of the number of p-α-Syn–positive cells and the number of TH-positive neuron loss were almost constant throughout the time course (Fig. 5b, e), suggesting the loss of α-Syn inclusion–bearing neurons. TH immunostaining in the dorsal striatum can be used to assess the degeneration of nigrostriatal dopaminergic neuron terminals [17, 29]. TH optical density in the dorsal striatum was not changed in the PBS-injected A53T BAC-*SNCA* Tg mice, whereas that was reduced by 42% in mPFF-injected A53T BAC-*SNCA* Tg mice at 0.5 month post-injection, without further reduction throughout the time course (Fig. 5c, f). We evaluated α-Syn pathology throughout the brains and found dynamic changes in the severity of the α-Syn pathology, depending on the brain region and time point (Fig. 5g, Additional file 3, 4: Figure S3, 4), which could be attributed to the combination of loss of α-Syn inclusion–bearing neurons and newly formed α-Syn pathology. We also examined glial involvement in this model. Iba1 immunostaining revealed an increased Iba1-positive area in the ipsilateral SNpc at 0.5 month post-injection, reflecting microglial activation (Fig. 6a, c). GFAP immunostaining also revealed trends toward an increase in the GFAP-positive area in the ipsilateral SNpc especially at 1 month post-injection, suggesting the possible involvement of reactive astrogliosis (Fig. 6b, d).

We also conducted pathological analyses on nTg mice injected with mPFFs up to 2 months post-injection and found a constant increase in the number of p-α-Syn–positive cells without obvious TH-positive neuron loss in the SNpc (Additional file 5: Figure S5a, b, d, e). These results further support the accelerated formation of α-Syn pathology and neuron loss in the mPFF-injected A53T BAC-*SNCA* Tg mice. Indeed, the mPFF-injected nTg mice at 2 months post-injection showed a similar number of p-α-Syn–positive cells and distribution of α-Syn pathology to those seen in the mPFF-injected A53T BAC-*SNCA* Tg mice at 0.5 month post-injection (Fig. 5d, g, Additional file 5: Figure S5d, g). TH optical density was reduced by 18% in the mPFF-injected nTg mice at 0.5 month post-injection, reaching a 30% reduction at 2 months post-injection (Additional file 5: Figure S5c, f). This suggests that the degeneration of dopaminergic neuron terminals is more severe in the mPFF-injected A53T BAC-*SNCA* Tg mice than in the mPFF-injected nTg mice and precedes dopaminergic neuron loss in the SNpc in both groups.

Behavioral features of mPFF-injected A53T BAC-SNCA Tg mice

We conducted a battery of behavioral analyses including an apomorphine-induced rotational behavior test on the mPFF-injected A53T BAC-*SNCA* Tg mice together with the PBS-injected nTg mice and PBS-injected A53T BAC-*SNCA* Tg mice as controls at 2 months post-injection. Apomorphine-induced rotational behavior test revealed an increased number of contralateral rotations (away from the injection side) in the mPFF-injected A53T BAC-*SNCA* Tg mice (Fig. 7a, b, Additional file 7–9: Video 1–3), suggesting dopamine hypersensitivity on the ipsilateral side [30]. Latency to fall in rotarod test and total distance in open field test were decreased in the mPFF-injected A53T BAC-*SNCA* Tg mice, even though both only attained statistical significance when comparing two groups, suggesting possible motor incoordination and reduced locomotion, respectively, in this model (Fig. 7c–e). Wire hang test revealed a decrease in latency to fall in the mPFF-injected A53T BAC-*SNCA* Tg mice, suggesting muscle weakness in this model (Fig. 7f). We also evaluated memory impairment, anxiety-like behavior, and depression-like behavior by other behavioral tests; however, we found no significant abnormalities in the mPFF-injected A53T BAC-*SNCA* Tg mice (Additional file 6: Figure. S6).

Discussion

In the present study, we applied striatal injection of two types of α-Syn PFFs, i.e., hPFFs and mPFFs, to two *SNCA* Tg mouse lines to generate a novel PD mouse model useful for the investigation of pathological mechanisms and drug testing. Among the groups we analyzed, the A53T BAC-*SNCA* Tg mice injected with mPFFs exhibited the most severe LB-like pathology as early as 0.5 month post-injection. These observations are consistent with our recent report about A53T BAC-*SNCA* Tg mice injected with mPFFs into the olfactory bulb [26]. The mPFF-injected A53T BAC-*SNCA* Tg mice exhibited motor dysfunction and a 38% reduction of dopaminergic neurons in the SNpc at 2 months post-injection. Given that many clinical trials evaluate the disease-modifying effects of candidate drugs by measuring changes in the UPDRS motor dysfunction scores at the endpoints, the motor dysfunction seen in this model within a short period after α-Syn PFF injection could be used as reliable indicators for exploring potential DMTs. Since the major pathological processes of this model are assumed to be neuronal uptake of α-Syn PFFs, templated fibrillization of α-Syn in neurons, interneuronal dissemination of pathological α-Syn aggregates, and α-Syn aggregation-induced neuron loss, the best application of this model would be testing candidate drugs intervening those processes. Of note, TH-immunoreactivity in the striatum and microglial activation in the SNpc was observed at 0.5 month post-injection, preceding obvious dopaminergic neuron loss.

Cross-seeded aggregation of human and mouse α-Syn is bidirectionally restricted, whereas seeded aggregation of α-Syn within the same host is efficiently induced [25]. However, it remains unclear how efficiently α-Syn aggregation could be induced by α-Syn PFF injection in *SNCA* Tg mice expressing both human and endogenous mouse α-Syn. In the present study, we tested two types of BAC-*SNCA* Tg mice and two types of α-Syn PFFs and identified the mPFF-injected A53T BAC-*SNCA* Tg mice as the model showing the most rapid formation of α-Syn pathology and subsequent neuron loss. However, there are possible ways to further accelerate the phenotypes of α-Syn PFF-injected mice. For instance, human S87N α-Syn PFFs were reported to show greater seeding activity in mouse primary neurons and WT mice

than mPFFs [25]. Previous studies reported that the deletion of endogenous mouse α-Syn exacerbated the α-Syn pathology in *SNCA* Tg mice [31, 32]. Therefore, it might be worth trying to use different types of PFFs and delete endogenous mouse α-Syn in BAC-*SNCA* Tg mice in future studies.

A previous study with a similar concept to that of the present study reported a rat PD model injected with α-Syn PFFs in combination with adeno-associated virus (AAV)-mediated overexpression of α-Syn [33]. The WT rats were first injected with human α-Syn–expressing AAV at a low dose in the SN and ventral tegmental area to avoid the induction of acute dopaminergic neuron loss. They subsequently received injection of human α-Syn PFFs into the same brain regions 4 weeks later, showing LB-like inclusions and a 55% reduction of dopaminergic neurons in the SN and impaired motor behavior 3 more weeks later. Both the rat model and our mouse model may have some advantages and disadvantages; the former methodology applies WT human α-Syn overexpression and PFFs that may replicate more faithfully pathobiology of sporadic PD, whereas two injections into the same brain regions may cause more severe tissue damage and more phenotypic variation among samples than our mouse model. Choosing the model for future studies depending on the purpose is necessary.

The reduction in TH density in the dorsal striatum is one of the earliest pathological changes in the mPFF-injected A53T BAC-*SNCA* Tg mice. There was a greater degree of reduction in TH density in the dorsal striatum than that in TH-positive neurons in the SNpc at 0.5 month post-injection. Similar observations have been reported by multiple studies carried out on subjects with PD. Loss of SN neurons and striatal dopamine terminals were estimated to be ~ 30% and ~ 70%, respectively, at the onset of motor symptoms [34]. Consistently, distal-dominant degeneration in Lewy pathology-bearing neurons has been reported. A previous study focusing on the cardiac sympathetic nervous system of cases with incidental LBs and subjects with PD revealed that the accumulation of α-Syn aggregates commences in the distal axons, followed by axonal degeneration and the formation of α-Syn aggregates in the somata and neurites [35]. In the present study, we conducted pathological analysis from 0.5 month post-injection, when robust p-α-Syn–positive somatic inclusions were already observed in the dopaminergic neurons of the SNpc in the mPFF-injected A53T BAC-*SNCA* Tg mice. Further details of degenerative processes should be examined at earlier time points in future studies.

Microglial activation has been well described in subjects with PD [36–38]. Lines of evidence have suggested that α-Syn–induced microglial activation plays both beneficial and detrimental roles in neurodegenerative processes. Activated microglia engulf neuron-released α-Syn into autophagosomes for degradation via selective autophagy, which protects against neurodegeneration [39]. Meanwhile, neuron-released oligomeric α-Syn induces neurotoxic microglial activation through Toll-like receptor 2 (TLR2) [40]. It has also been demonstrated that recombinant monomeric, C-terminal, and fibrillar α-Syn are phagocytosed through TLR4 by microglia, inducing proinflammatory cytokine release and reactive oxygen species production [41]. In the present study, microglial activation was observed before obvious dopaminergic neuron loss in the mPFF-injected A53T BAC-*SNCA* Tg mice, suggesting that microglia may play some roles in the degenerative processes in this model. In this regard, some interventions on microglial functions could be also tested in this model.

Conclusions

We generated a novel mouse model which recapitulates several pathological and behavioral features of PD within a short period by applying α-Syn PFF injection to A53T BAC-*SNCA* Tg mice. This novel model will be useful in the development of DMTs as well as the investigation of pathological mechanisms in PD research.

Abbreviations

PD, Parkinson's disease; SNpc, substantia nigra pars compacta; α-Syn, α-Synuclein; LBs, Lewy bodies; DMTs, disease-modifying therapies; PFFs, preformed fibrils; hPFFs, human α-Syn preformed fibrils; mPFFs, mouse α-Syn preformed fibrils; WT BAC-*SNCA* Tg, wild-type human α-Syn BAC transgenic; A53T BAC-*SNCA* Tg, A53T human α-Syn BAC transgenic; TH, tyrosine hydroxylase; UPDRS, Unified Parkinson's Disease Rating Scale; WT, wild-type; BAC, bacterial artificial chromosome; RBD, REM sleep behavior disorder; nTg, non-transgenic; PBS, phosphate buffer saline; SDS, sodium dodecyl sulfate; PFA, paraformaldehyde; p-α-Syn, phosphorylated-α-Syn; Iba1, ionized calcium-binding adapter molecule 1; GFAP, glial fibrillary acidic protein; CS, conditioned stimulus; US, unconditioned stimulus; AAV, adeno-associated virus; TLR, Toll-like receptor; BLA, basolateral amygdala; Ent, entorhinal cortex; mpi, month post-injection; Ctx, motor cortex; nTg-PBS, nTg mice injected with PBS; A53T-PBS, A53T BAC-*SNCA* Tg mice injected with PBS; A53T-mPFF, A53T BAC-*SNCA* Tg mice injected with mPFFs; CA1, cornu ammonis 1

Declarations

Ethics approval and consent to participate

Details of ethical approval, and permission about animal research are described in "Methods." All applicable international, national, and/or institutional guidelines for the welfare and usage of animals were followed.

Consent for publication

Not applicable.

Availability of data and materials

The data and materials that support the findings of this study are available from the corresponding authors upon reasonable request.

Competing interests

The authors declare that they have no conflict of interest.

Funding

This research is supported by the program for Brain Mapping by Integrated Neurotechnologies for Disease Studies (Brain/MINDS) from Ministry of Education, Culture, Sports Science, MEXT, and the Japan Agency for Medical Research and Development, AMED under the Grant Numbers JP18dm0207020 and JP20dm0207070 (RT), JSPS KAKENHI Grant Number JP17H05698 and JP18H04041 (RT).

Authors' contributions

SO conceived the study, performed the experiments, analyzed the data, and wrote the manuscript. NU conceived the study, analyzed the data, and wrote the manuscript. MS analyzed the data. TT, MI, and MTU generated and provided the transgenic mice. HY supervised the study. RT supervised the study and edited the manuscript. All authors read and approved the final manuscript.

Acknowledgements

We thank Ms. Rie Hikawa for the technical assistance.

References

1. Kalia LV, Lang AE: **Parkinson's disease.***The Lancet* 2015, **386:**896-912.
2. Hely MA, Reid WG, Adena MA, Halliday GM, Morris JG: **The Sydney multicenter study of Parkinson's disease: the inevitability of dementia at 20 years.***Mov Disord* 2008, **23:**837-844.
3. Greffard S, Verny M, Bonnet AM, Beinis JY, Gallinari C, Meaume S, Piette F, Hauw JJ, Duyckaerts C: **Motor score of the Unified Parkinson Disease Rating Scale as a good predictor of Lewy body-associated neuronal loss in the substantia nigra.***Archives of neurology* 2006, **63:**584-588.
4. Irwin DJ, White MT, Toledo JB, Xie SX, Robinson JL, Van Deerlin V, Lee VM, Leverenz JB, Montine TJ, Duda JE, et al: **Neuropathologic substrates of Parkinson disease dementia.***Ann Neurol* 2012, **72:**587-598.
5. Hall H, Reyes S, Landeck N, Bye C, Leanza G, Double K, Thompson L, Halliday G, Kirik D: **Hippocampal Lewy pathology and cholinergic dysfunction are associated with dementia in Parkinson's disease.***Brain* 2014, **137:**2493-2508.
6. Churchyard A, Lees AJ: **The relationship between dementia and direct involvement of the hippocampus and amygdala in Parkinson's disease.***Neurology* 1997, **49:**1570-1576.
7. Koprich JB, Kalia LV, Brotchie JM: **Animal models of α-synucleinopathy for Parkinson disease drug development.***Nat Rev Neurosci* 2017, **18:**515-529.
8. Salamon A, Zádori D, Szpisjak L, Klivényi P, Vécsei L: **Neuroprotection in Parkinson's disease: facts and hopes.***Journal of neural transmission (Vienna, Austria : 1996)* 2020, **127:**821-829.
9. Polymeropoulos MH, Lavedan C, Leroy E, Ide SE, Dehejia A, Dutra A, Pike B, Root H, Rubenstein J, Boyer R, et al: **Mutation in the alpha-synuclein gene identified in families with Parkinson's**

disease.*Science* 1997, **276:**2045-2047.

10. Singleton AB, Farrer M, Johnson J, Singleton A, Hague S, Kachergus J, Hulihan M, Peuralinna T, Dutra A, Nussbaum R, et al: **alpha-Synuclein locus triplication causes Parkinson's disease.***Science* 2003, **302:**841.
11. Chartier-Harlin MC, Kachergus J, Roumier C, Mouroux V, Douay X, Lincoln S, Levecque C, Larvor L, Andrieux J, Hulihan M, et al: **Alpha-synuclein locus duplication as a cause of familial Parkinson's disease.***Lancet (London, England)* 2004, **364:**1167-1169.
12. Ibáñez P, Bonnet AM, Débarges B, Lohmann E, Tison F, Pollak P, Agid Y, Dürr A, Brice A: **Causal relation between alpha-synuclein gene duplication and familial Parkinson's disease.***Lancet (London, England)* 2004, **364:**1169-1171.
13. Visanji NP, Brotchie JM, Kalia LV, Koprich JB, Tandon A, Watts JC, Lang AE: **α-Synuclein-Based Animal Models of Parkinson's Disease: Challenges and Opportunities in a New Era.***Trends Neurosci* 2016, **39:**750-762.
14. Decressac M, Mattsson B, Lundblad M, Weikop P, Björklund A: **Progressive neurodegenerative and behavioural changes induced by AAV-mediated overexpression of α-synuclein in midbrain dopamine neurons.***Neurobiology of disease* 2012, **45:**939-953.
15. Van der Perren A, Toelen J, Casteels C, Macchi F, Van Rompuy AS, Sarre S, Casadei N, Nuber S, Himmelreich U, Osorio Garcia MI, et al: **Longitudinal follow-up and characterization of a robust rat model for Parkinson's disease based on overexpression of alpha-synuclein with adeno-associated viral vectors.***Neurobiology of aging* 2015, **36:**1543-1558.
16. Uemura N, Uemura MT, Luk KC, Lee VM, Trojanowski JQ: **Cell-to-Cell Transmission of Tau and α-Synuclein.***Trends in molecular medicine* 2020.
17. Luk KC, Kehm V, Carroll J, Zhang B, O'Brien P, Trojanowski JQ, Lee VM: **Pathological alpha-synuclein transmission initiates Parkinson-like neurodegeneration in nontransgenic mice.***Science* 2012, **338:**949-953.
18. Masuda-Suzukake M, Nonaka T, Hosokawa M, Oikawa T, Arai T, Akiyama H, Mann DM, Hasegawa M: **Prion-like spreading of pathological alpha-synuclein in brain.***Brain* 2013, **136:**1128-1138.
19. Yamakado H, Moriwaki Y, Yamasaki N, Miyakawa T, Kurisu J, Uemura K, Inoue H, Takahashi M, Takahashi R: **alpha-Synuclein BAC transgenic mice as a model for Parkinson's disease manifested decreased anxiety-like behavior and hyperlocomotion.***Neurosci Res* 2012, **73:**173-177.
20. Taguchi T, Ikuno M, Hondo M, Parajuli LK, Taguchi K, Ueda J, Sawamura M, Okuda S, Nakanishi E, Hara J, et al: **α-Synuclein BAC transgenic mice exhibit RBD-like behaviour and hyposmia: a prodromal Parkinson's disease model.***Brain* 2020, **143:**249-265.
21. Ikuno M, Yamakado H, Akiyama H, Parajuli LK, Taguchi K, Hara J, Uemura N, Hatanaka Y, Higaki K, Ohno K, et al: **GBA haploinsufficiency accelerates alpha-synuclein pathology with altered lipid metabolism in a prodromal model of Parkinson's disease.***Hum Mol Genet* 2019, **28:**1894-1904.
22. Uemura N, Uemura MT, Lo A, Bassil F, Zhang B, Luk KC, Lee VM, Takahashi R, Trojanowski JQ: **Slow Progressive Accumulation of Oligodendroglial Alpha-Synuclein (alpha-Syn) Pathology in Synthetic**

alpha-Syn Fibril-Induced Mouse Models of Synucleinopathy.*Journal of neuropathology and experimental neurology* 2019, **78:**877-890.

23. Uemura N, Yagi H, Uemura MT, Hatanaka Y, Yamakado H, Takahashi R: **Inoculation of alpha-synuclein preformed fibrils into the mouse gastrointestinal tract induces Lewy body-like aggregates in the brainstem via the vagus nerve.***Molecular neurodegeneration* 2018, **13:**21.
24. Uemura N, Yagi H, Uemura MT, Yamakado H, Takahashi R: **Limited spread of pathology within the brainstem of alpha-synuclein BAC transgenic mice inoculated with preformed fibrils into the gastrointestinal tract.***Neuroscience letters* 2020, **716:**134651.
25. Luk KC, Covell DJ, Kehm VM, Zhang B, Song IY, Byrne MD, Pitkin RM, Decker SC, Trojanowski JQ, Lee VM: **Molecular and Biological Compatibility with Host Alpha-Synuclein Influences Fibril Pathogenicity.***Cell reports* 2016, **16:**3373-3387.
26. Uemura N, Ueda J, Yoshihara T, Ikuno M, Uemura MT, Yamakado H, Asano M, Trojanowski JQ, Takahashi R: **α-Synuclein Spread from Olfactory Bulb Causes Hyposmia, Anxiety, and Memory Loss in BAC-SNCA Mice.***Mov Disord* 2021.
27. da Conceição FS, Ngo-Abdalla S, Houzel JC, Rehen SK: **Murine model for Parkinson's disease: from 6-OH dopamine lesion to behavioral test.***Journal of visualized experiments : JoVE* 2010.
28. Osterberg VR, Spinelli KJ, Weston LJ, Luk KC, Woltjer RL, Unni VK: **Progressive aggregation of alpha-synuclein and selective degeneration of lewy inclusion-bearing neurons in a mouse model of parkinsonism.***Cell reports* 2015, **10:**1252-1260.
29. Kordower JH, Olanow CW, Dodiya HB, Chu Y, Beach TG, Adler CH, Halliday GM, Bartus RT: **Disease duration and the integrity of the nigrostriatal system in Parkinson's disease.***Brain* 2013, **136:**2419-2431.
30. Bové J, Perier C: **Neurotoxin-based models of Parkinson's disease.***Neuroscience* 2012, **211:**51-76.
31. Cabin DE, Gispert-Sanchez S, Murphy D, Auburger G, Myers RR, Nussbaum RL: **Exacerbated synucleinopathy in mice expressing A53T SNCA on a Snca null background.***Neurobiology of aging* 2005, **26:**25-35.
32. Fares MB, Maco B, Oueslati A, Rockenstein E, Ninkina N, Buchman VL, Masliah E, Lashuel HA: **Induction of de novo α-synuclein fibrillization in a neuronal model for Parkinson's disease.***Proc Natl Acad Sci U S A* 2016, **113:**E912-921.
33. Thakur P, Breger LS, Lundblad M, Wan OW, Mattsson B, Luk KC, Lee VMY, Trojanowski JQ, Björklund A: **Modeling Parkinson's disease pathology by combination of fibril seeds and α-synuclein overexpression in the rat brain.***Proc Natl Acad Sci U S A* 2017, **114:**E8284-e8293.
34. Cheng HC, Ulane CM, Burke RE: **Clinical progression in Parkinson disease and the neurobiology of axons.***Ann Neurol* 2010, **67:**715-725.
35. Orimo S, Uchihara T, Nakamura A, Mori F, Kakita A, Wakabayashi K, Takahashi H: **Axonal alpha-synuclein aggregates herald centripetal degeneration of cardiac sympathetic nerve in Parkinson's disease.***Brain* 2008, **131:**642-650.

36. McGeer PL, Itagaki S, Akiyama H, McGeer EG: **Rate of cell death in parkinsonism indicates active neuropathological process.***Ann Neurol* 1988, **24:**574-576.
37. Imamura K, Hishikawa N, Sawada M, Nagatsu T, Yoshida M, Hashizume Y: **Distribution of major histocompatibility complex class II-positive microglia and cytokine profile of Parkinson's disease brains.***Acta neuropathologica* 2003, **106:**518-526.
38. Croisier E, Moran LB, Dexter DT, Pearce RK, Graeber MB: **Microglial inflammation in the parkinsonian substantia nigra: relationship to alpha-synuclein deposition.***Journal of neuroinflammation* 2005, **2:**14.
39. Choi I, Zhang Y, Seegobin SP, Pruvost M, Wang Q, Purtell K, Zhang B, Yue Z: **Microglia clear neuron-released α-synuclein via selective autophagy and prevent neurodegeneration.***Nat Commun* 2020, **11:**1386.
40. Kim C, Ho DH, Suk JE, You S, Michael S, Kang J, Joong Lee S, Masliah E, Hwang D, Lee HJ, Lee SJ: **Neuron-released oligomeric alpha-synuclein is an endogenous agonist of TLR2 for paracrine activation of microglia.***Nat Commun* 2013, **4:**1562.
41. Fellner L, Irschick R, Schanda K, Reindl M, Klimaschewski L, Poewe W, Wenning GK, Stefanova N: **Toll-like receptor 4 is required for α-synuclein dependent activation of microglia and astroglia.***Glia* 2013, **61:**349-360.

Figures

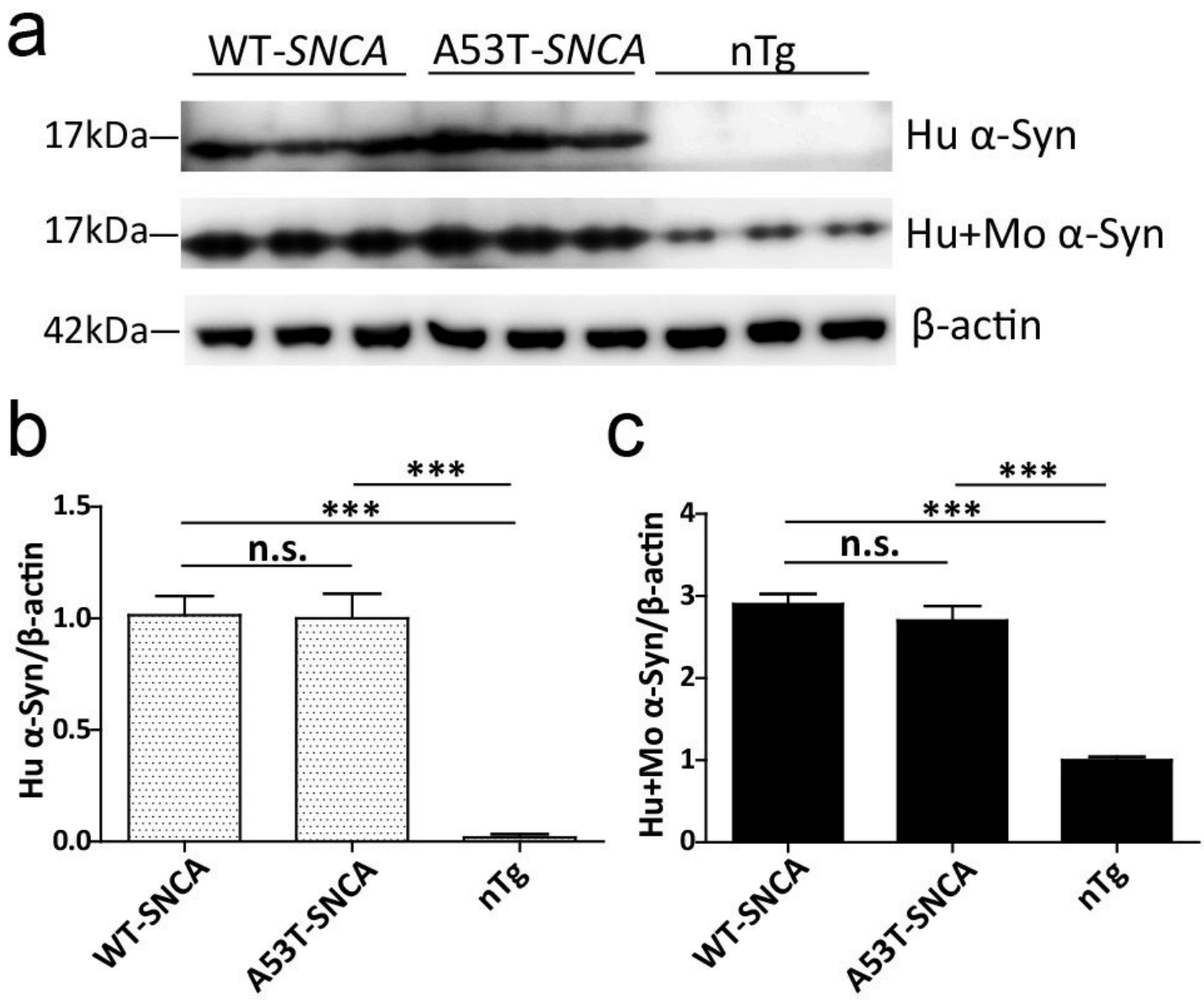

Figure 1

α-Syn expression in the brains of WT BAC-SNCA Tg and A53T BAC-SNCA Tg mice. (a) Western blot analysis of whole brain lysates of WT BAC-SNCA Tg (WT-SNCA), A53T BAC-SNCA Tg (A53T-SNCA), and nTg mice with LB509 (human [Hu] α-Syn) and Syn-1 (human and mouse [Mo] α-Syn) antibodies. (b, c) Quantification of LB509 and Syn-1–positive bands normalized by β-actin (n = 3). Results are shown as values relative to A53T-SNCA (b) and nTg (c). One-way ANOVA with Tukey's post hoc test was performed; ***$p < 0.001$; n.s., not significant. Data are the mean ± SEM.

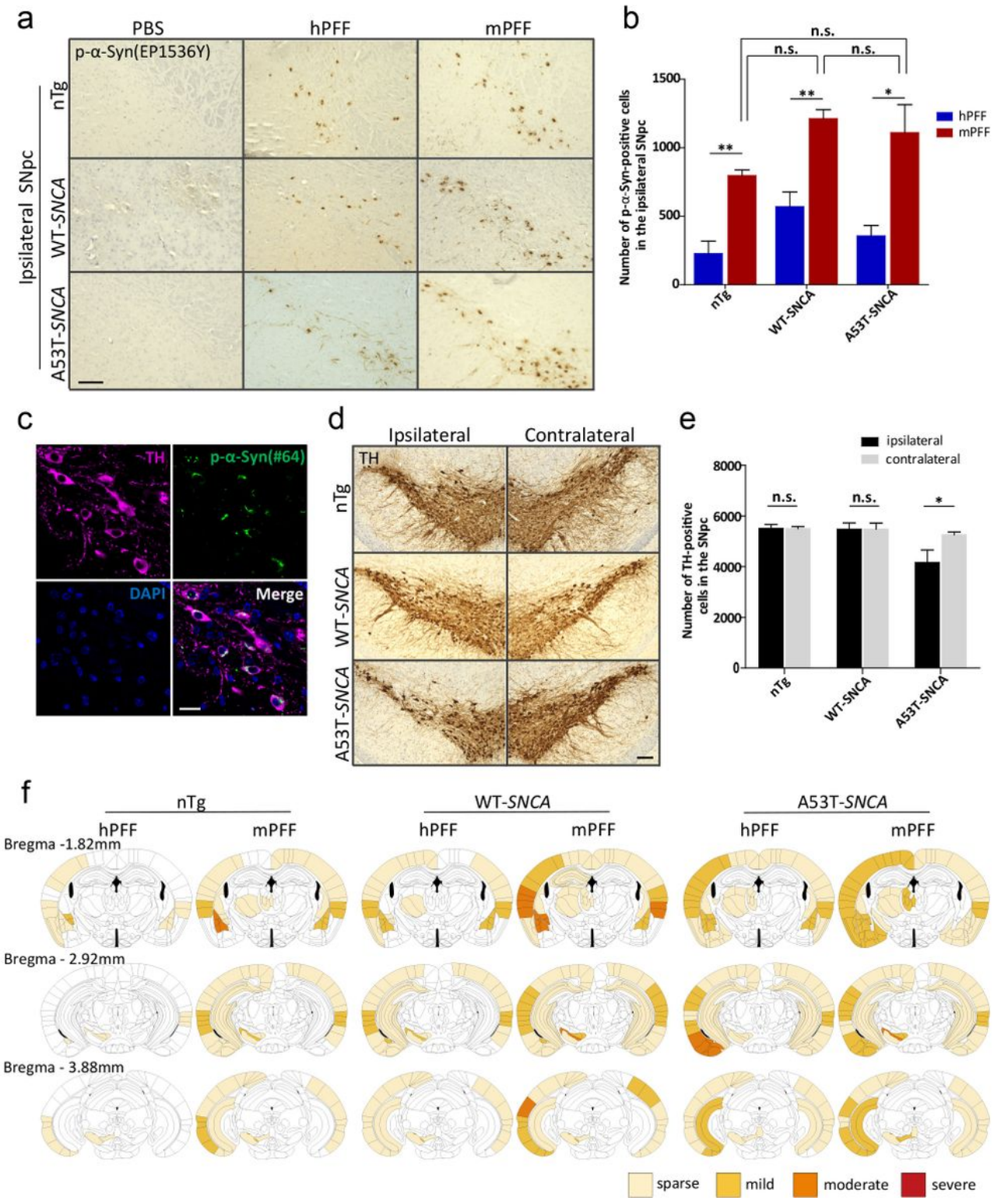

Figure 2

Comparisons of pathological changes among hPFF-, mPFF-, and PBS-injected mice at 1 month post-injection. (a) P-α-Syn (EP1536Y) immunostaining of the ipsilateral SNpc. Scale bar 100 μm. (b) Number of p-α-syn–positive cells in the ipsilateral SNpc (n = 3–4). A two-tailed Student's t-test was performed within each genotype; *p < 0.05, **p < 0.01. One-way ANOVA with Tukey's post hoc test was performed among mPFF-injected groups; n.s., not significant. (c) Double immunostaining for TH and p-α-Syn (#64)

in the ipsilateral SNpc of mPFF-injected A53T BAC-SNCA Tg mice. Scale bar 20 μm. (d) TH immunostaining of the SNpc of mPFF-injected mice. Scale bar 100 μm. (e) Number of TH-positive cells in the SNpc of mPFF-injected mice (n = 3–4). A two-tailed Student's t-test was performed within each genotype; *p < 0.05; n.s., not significant. Data are mean ± SEM. (f) Heat map colors represent the extent of α-Syn pathology (light yellow, sparse pathology; yellow, mild pathology; orange, moderate pathology; red, severe pathology). Left is the injection (ipsilateral) side.

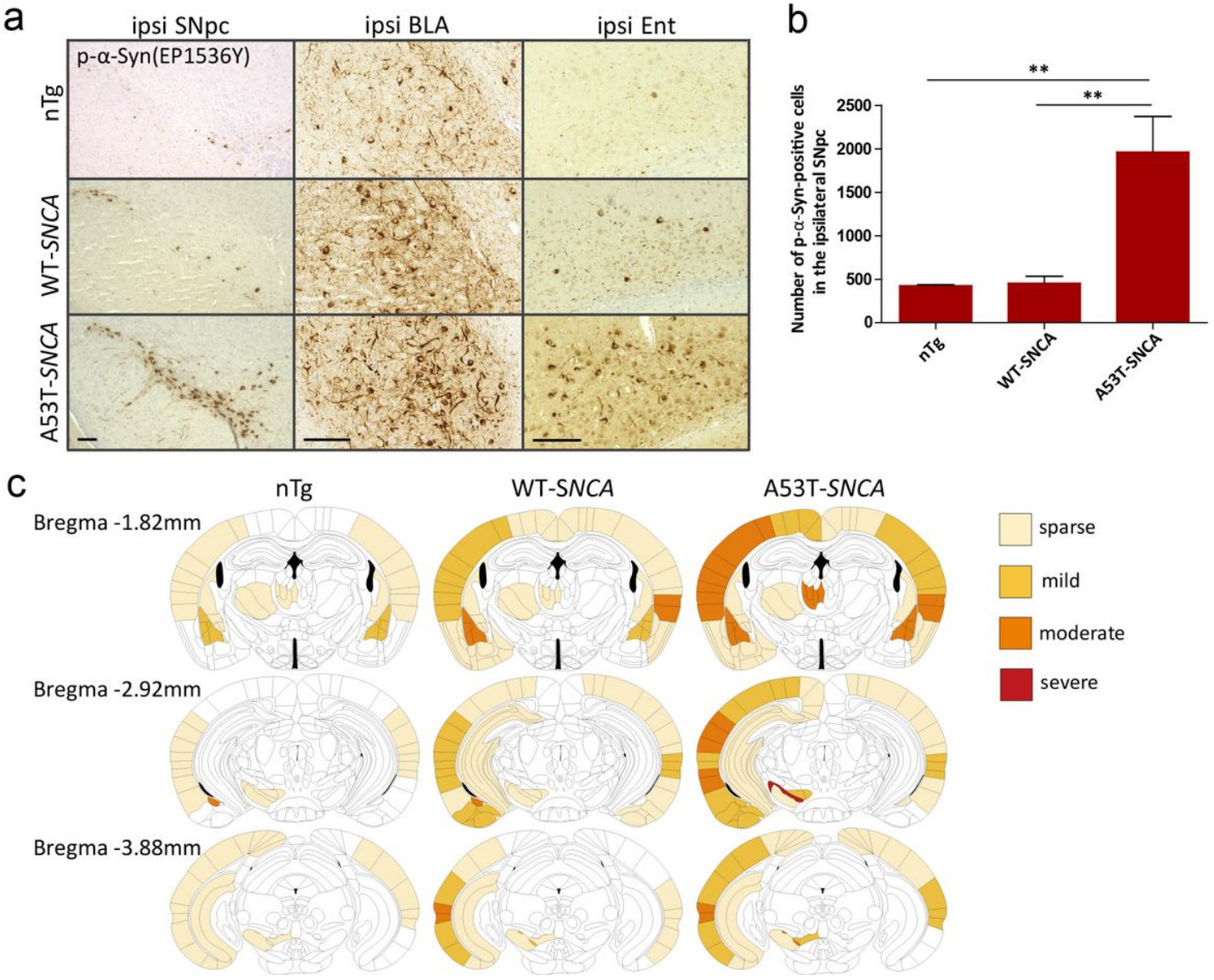

Figure 3

Comparisons of pathological changes in the mPFF-injected mice at 0.5 month post-injection. (a) P-α-Syn (EP1536Y) immunostaining of the ipsilateral SNpc, basolateral amygdala (BLA) and entorhinal cortex (Ent) of mPFF-injected mice. Scale bar 100 μm. (b) Number of p-α-Syn–positive cells in the ipsilateral SNpc of mPFF-injected mice (n = 3–4). One-way ANOVA with Tukey's post hoc test was performed; **p < 0.01. Data are the mean ± SEM. (c) Heat map colors represent the extent of α-Syn pathology (light yellow,

sparse pathology; yellow, mild pathology; orange, moderate pathology; red, severe pathology). Left is the injection (ipsilateral) side.

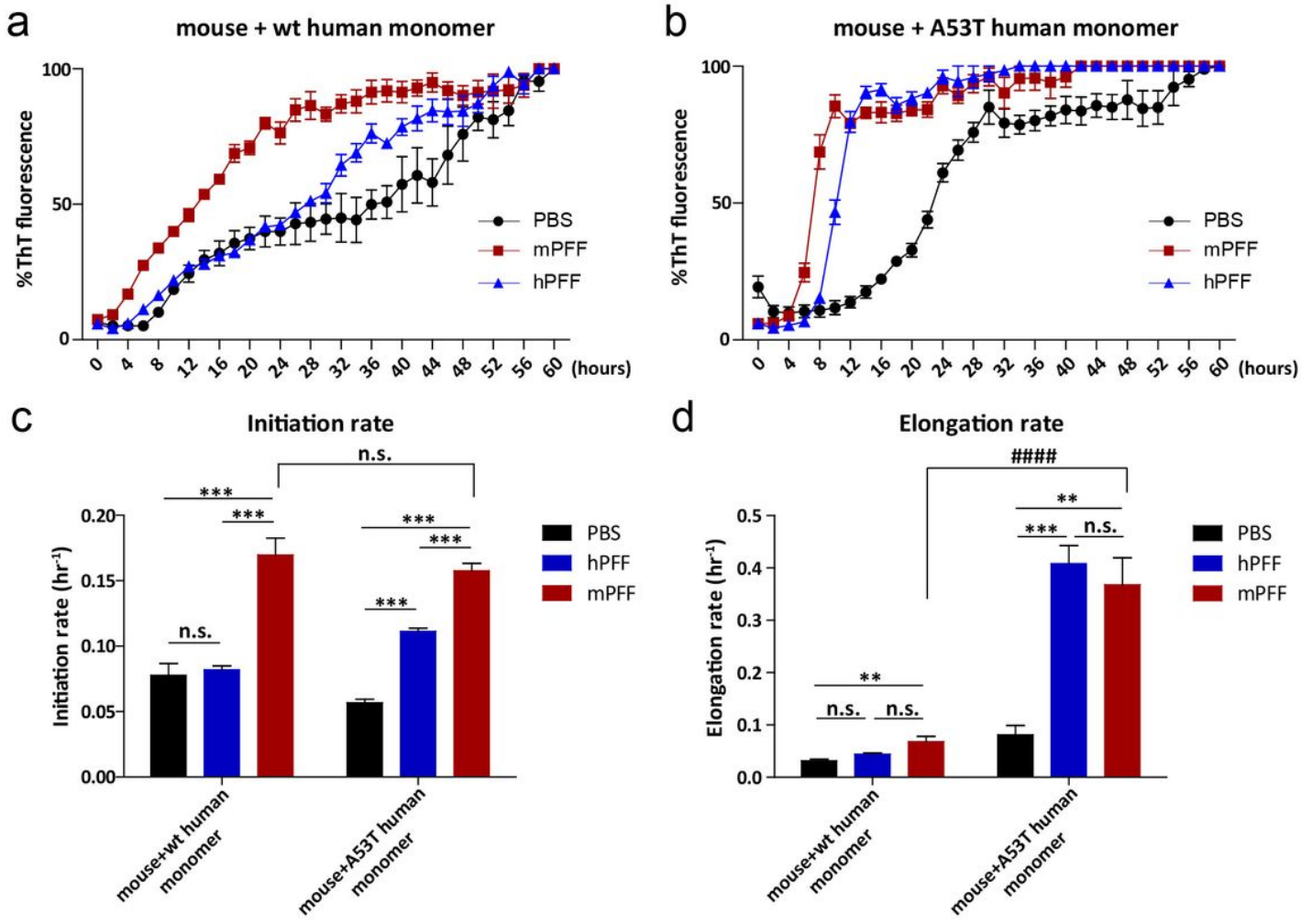

Figure 4

A53T human α-Syn fibrillizes more rapidly than WT human α-Syn in the presence of mouse α-Syn in in vitro α-Syn fibrillization assay. (a, b) Mixture of mouse α-Syn and WT or A53T human α-Syn monomers seeded with hPFFs, mPFFs, or PBS and then constantly agitated. Fluorescence of thioflavin T was plotted every 2 h (n = 4). (c) Initiation rates represent the inverse values of time to reach 25% of the maximum fluorescence. (d) Elongation rates represent the inverse values of time from 25% to 75% of the maximum fluorescence. One-way ANOVA with Tukey's post hoc test was performed among mixture of mouse α-Syn and WT or A53T human α-Syn monomer groups; **p < 0.01, ***p < 0.001; n.s., not significant. A two-tailed Student's t-test was performed within mPFF-seeded groups; ####p < 0.0001; n.s., not significant. Data are the mean ± SEM.

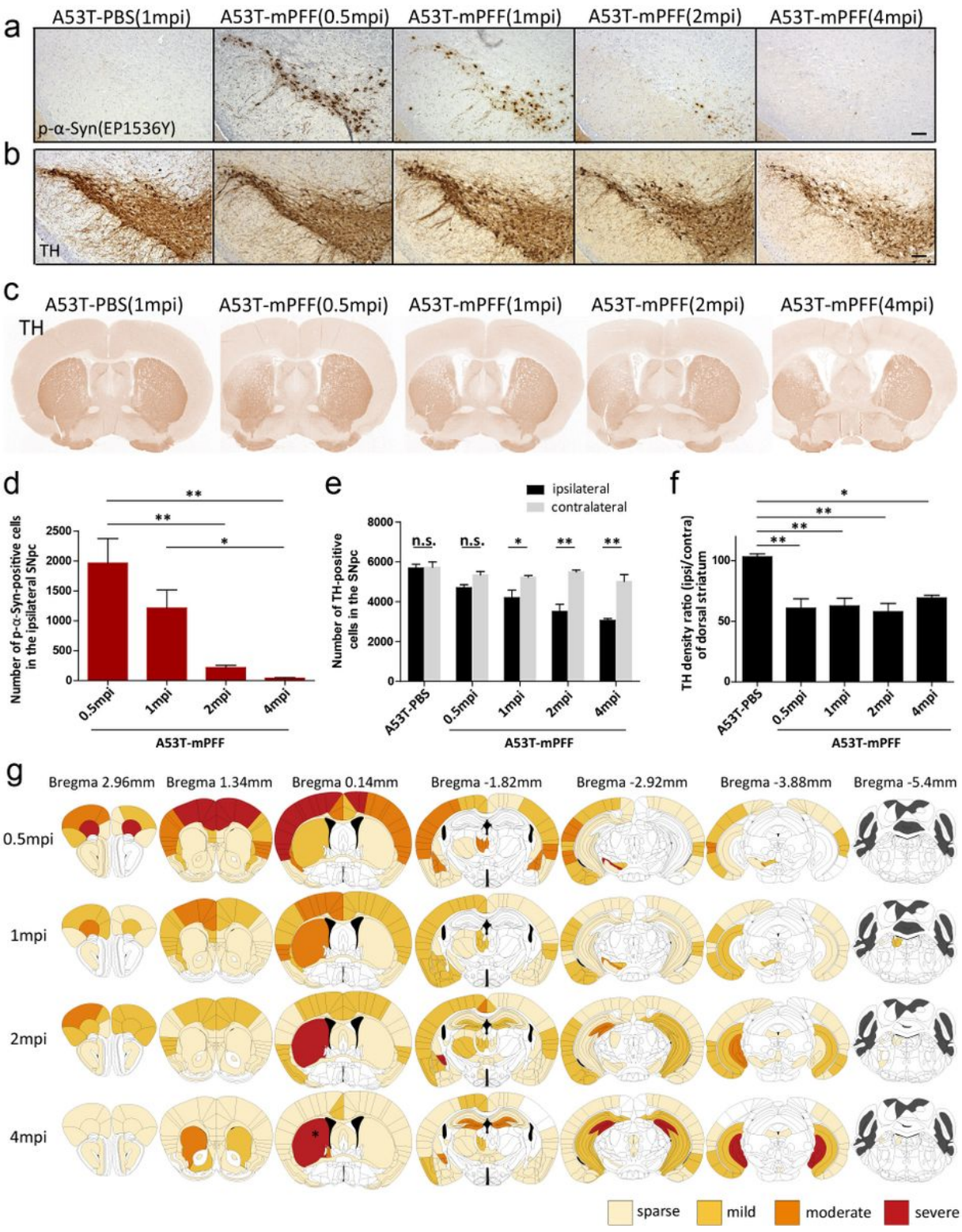

Figure 5

Pathological characterization of the mPFF-injected A53T BAC-SNCA Tg mice. A53T BAC-SNCA Tg mice injected with mPFFs (A53T-mPFF) or PBS (A53T-PBS). Month post-injection is abbreviated as mpi. (a, b) P-α-Syn (EP1536Y) and TH immunostaining of the ipsilateral SNpc. Scale bar 100 μm. (c) TH immunostaining of the striatum. Left is the injection (ipsilateral) side. (d) Number of p-α-Syn–positive cells in the ipsilateral SNpc (n = 3–5). One-way ANOVA with Tukey's post hoc test was performed; *p <

0.05, **p < 0.01. (e) Number of TH-positive cells in the ipsilateral and contralateral SNpc (n = 3–5). A two-tailed Student's t-test was performed within each time point; *p < 0.05, **p < 0.01; n.s., not significant. (f) TH optical density ratio of ipsilateral to contralateral side of the dorsal striatum (n = 3–5). One-way ANOVA with Tukey's post hoc test was performed; *p < 0.05, **p < 0.01. (g) Heat map colors represent the extent of α-Syn pathology (light yellow, sparse pathology; yellow, mild pathology; orange, moderate pathology; red, severe pathology). Asterisks indicate the injection sites. Data are mean ± SEM.

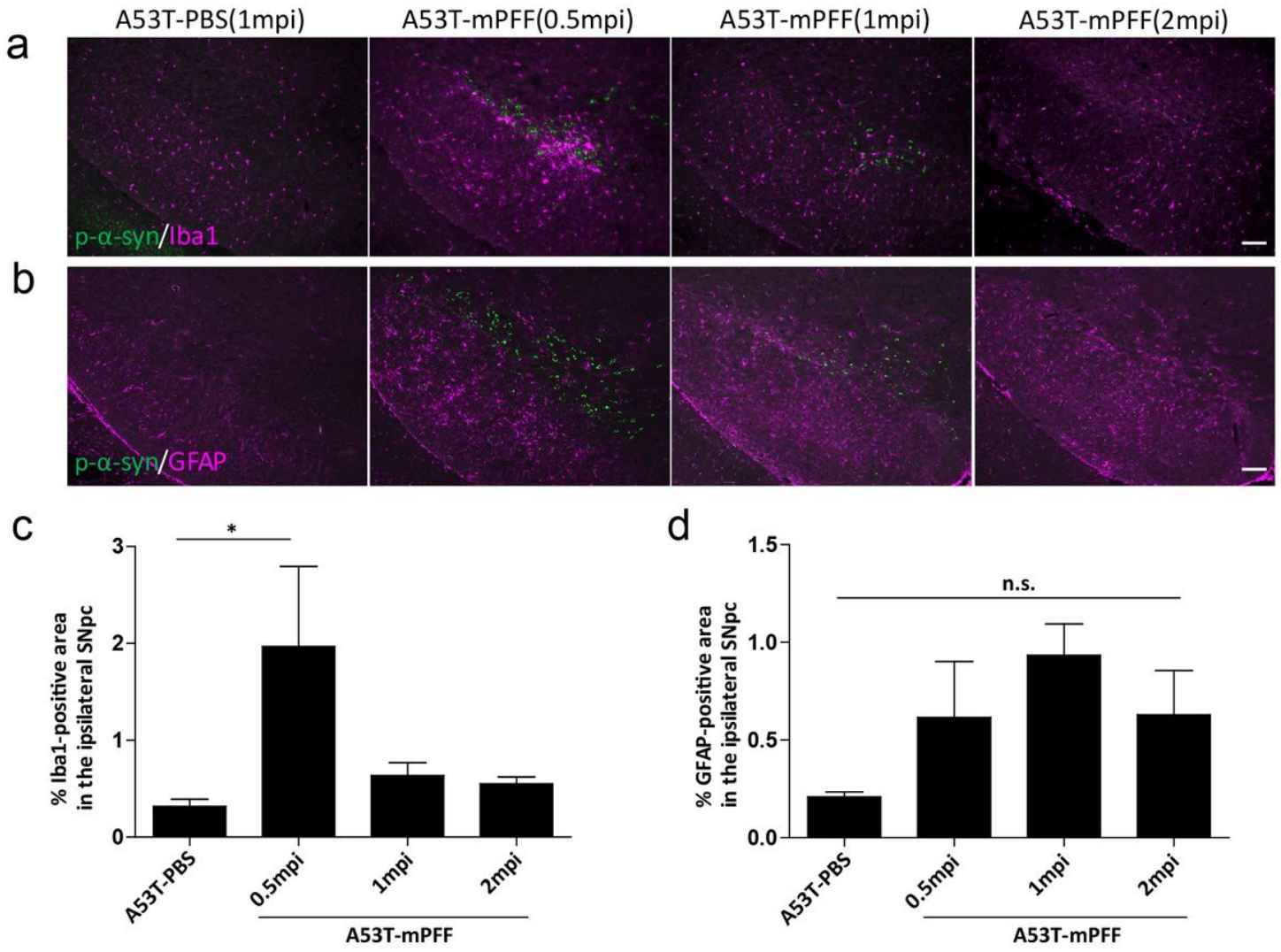

Figure 6

Microglial activation and reactive astrogliosis in the ipsilateral SNpc of the mPFF-injected A53T BAC-SNCA Tg mice. (a) Double immunostaining for p-α-Syn (#64) and Iba1 in the SNpc of mPFF-injected A53T BAC-SNCA Tg mice. Scale bar 100 μm. (b) Double immunostaining for p-α-Syn (EP1536Y) and GFAP in the SNpc of mPFF-injected A53T BAC-SNCA Tg mice. Scale bar 100 μm. (c) Percentage of Iba1-positive area in the ipsilateral SNpc of mPFF-injected A53T BAC-SNCA Tg mice. Kruskal-Wallis test with Dunn's post hoc test was performed; *p < 0.05. (d) Percentage of GFAP-positive area in the ipsilateral SNpc of mPFF-injected A53T BAC-SNCA Tg mice. Kruskal-Wallis test was performed; n.s., not significant.

Comparing A53T-PBS and A53T-mPFF 1mpi, a two-tailed unpaired Student's t-test showed unadjusted p = 0.011. Data are the mean ± SEM.

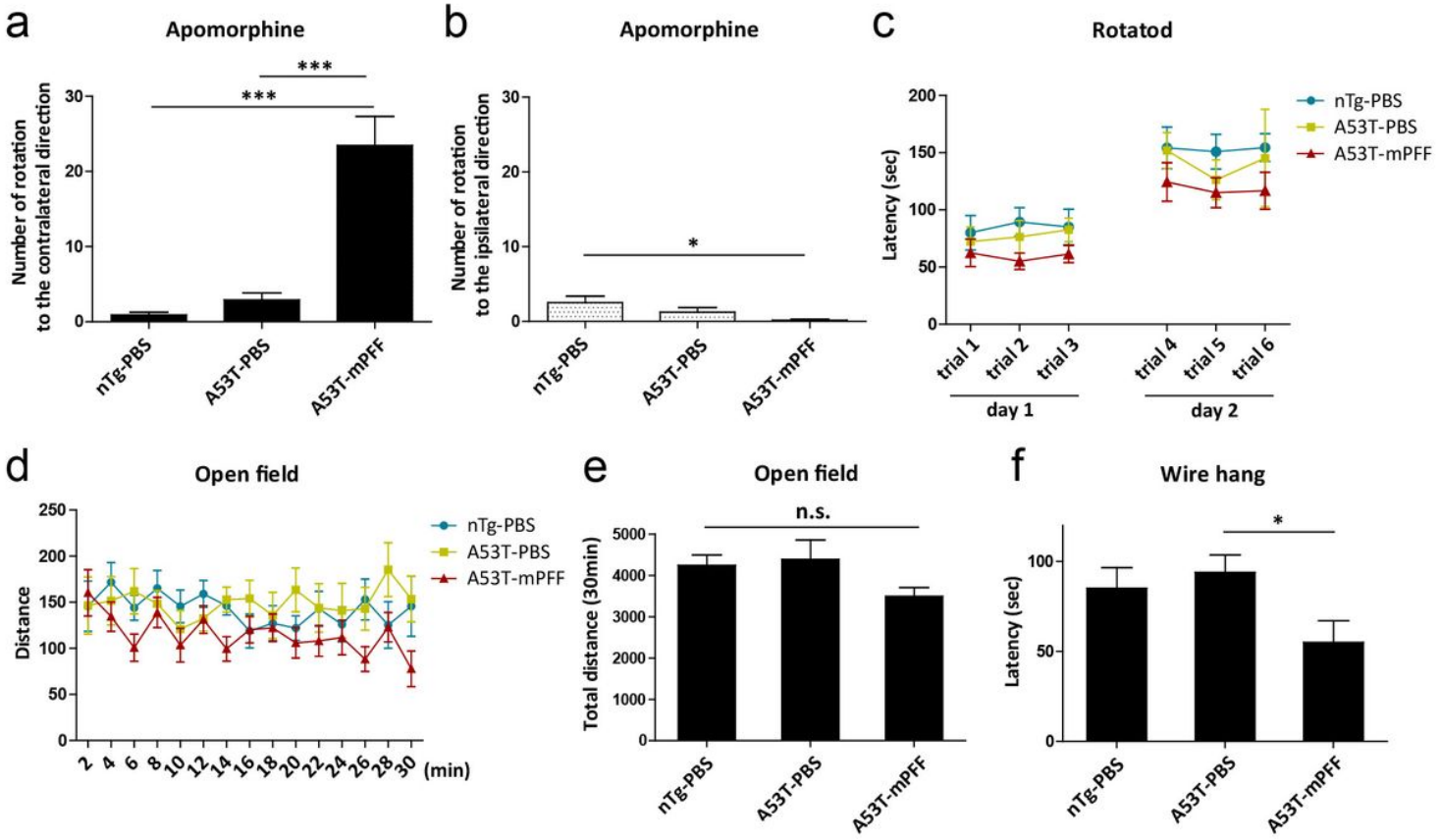

Figure 7

Behavioral abnormalities in the mPFF-injected A53T BAC-SNCA Tg mice. nTg mice injected with PBS (nTg-PBS), A53T BAC-SNCA Tg mice injected with PBS (A53T-PBS) and A53T BAC-SNCA Tg mice injected with mPFFs (A53T-mPFF) at 2 months post-injection (n = 12–13). (a, b) Number of rotations to the contralateral and ipsilateral directions in apomorphine-induced rotational behavior test. One-way ANOVA with Tukey's post hoc test was performed; *p < 0.05, ***p < 0.001. (c) Latency to fall in rotarod test. Two-way repeated measures (RM) ANOVA was performed; Comparing three groups, effect of group, $F_{2,35}$ = 2.609, p = 0.088. Comparing A53T-mPFF with nTg-PBS, effect of group, $F_{1,23}$ = 5.814, p = 0.024. (d, e) Open field test. (d) Moving distance plotted every 2 min. Two-way RM ANOVA was performed; Comparing three groups, effect of group, $F_{2,35}$ = 2.101, p = 0.138. Comparing A53T-mPFF with nTg-PBS, effect of group, $F_{1,23}$ = 5.31, unadjusted p = 0.031. (e) Total distance. One-way ANOVA with Tukey's post hoc test was performed; n.s., not significant. Comparing A53T-mPFF with nTg-PBS, a two-tailed unpaired Student's t-test showed unadjusted p = 0.031. (f) Latency to fall in wire hang test. One-way ANOVA with Tukey's post hoc test was performed; *p < 0.05. Data are the mean ± SEM.

Supplementary Files

This is a list of supplementary files associated with this preprint. Click to download.

- Additionalfile1.pdf
- Additionalfile2.pdf
- Additionalfile3.pdf
- Additionalfile4.pdf
- Additionalfile5.pdf
- Additionalfile6.pdf
- Additionalfile7.mp4
- Additionalfile8.mp4
- Additionalfile9.mp4